

¹ Open-Source Hypothalamic-ForniX (OSHy-X) Atlases and ² Segmentation Tool for 3T and 7T

³ **Jeryn Chang^{1¶}, Frederik Steyn^{1,2,3,4}, Shyuan Ngo^{2,3,4,5}, Robert**
⁴ **Henderson^{2,3,4}, Christine Guo⁶, Steffen Bollmann^{7,8}, Jurgen Fripp⁹,**
⁵ **Markus Barth^{7,8}, and Thomas Shaw^{2,7,8}**

⁶ 1 School of Biomedical Sciences, The University of Queensland 2 Department of Neurology, Royal
⁷ Brisbane and Women's Hospital, Australia 3 Wesley Medical Research, The Wesley Hospital 4 UQ
⁸ Centre for Clinical Research, The University of Queensland 5 Australian Institute of Bioengineering
⁹ and Nanotechnology, The University of Queensland 6 ActiGraph, LLC, Pensacola, FL, USA 7 Centre
¹⁰ for Advanced Imaging, The University of Queensland 8 School of Information Technology and
¹¹ Electrical Engineering, The University of Queensland 9 CSIRO Health and Biosecurity, The Australian
¹² eHealth Research Centre, Brisbane, Australia ¶ Corresponding author

DOI: [10.xxxxxx/draft](https://doi.org/10.xxxxxx/draft)

Software

- [Review ↗](#)
- [Repository ↗](#)
- [Archive ↗](#)

Editor: ↗

Submitted: 11 April 2022

Published: unpublished

License

Authors of papers retain
copyright and release the work
under a Creative Commons
Attribution 4.0 International
License ([CC BY 4.0](https://creativecommons.org/licenses/by/4.0/)).

¹³ Summary

¹⁴ Segmentation and volumetric analysis of the hypothalamus and fornix plays a critical role in
¹⁵ improving the understanding of degenerative processes that might impact the function of these
¹⁶ structures. We present Open-Source Hypothalamic-ForniX (OSHy-X) atlases and tool for multi-
¹⁷ atlas fusion segmentation for 3T and 7T. The atlases are based on 20 manual segmentations,
¹⁸ which we demonstrate have high interrater agreement. The versatility of the OSHy-X tool allows
¹⁹ segmentation and volumetric analysis of the hypothalamus and fornix from MRI scans. We
²⁰ also demonstrate that OSHy-X segmentation outperforms a deep-learning segmentation method
²¹ for the hypothalamus ([Billot et al., 2020](#)). We have previously demonstrated the use of OSHy-X
²² on a cohort of 329 non-neurodegenerative control participants and 42 patients with ALS to
²³ investigate reduced hypothalamic volume and its association with appetite, hypermetabolism
²⁴ and weight loss ([Chang et al., 2022](#)).

²⁵ Statement of need

²⁶ Segmentation of small structures of the brain including the hypothalamus and fornix is
²⁷ important for primary research of health and disease. One such disease that has implications
²⁸ for the volume of the hypothalamus is Amyotrophic Lateral Sclerosis (ALS). ALS is a fatal
²⁹ neurodegenerative disease that involves the degeneration and death of motor neurons in the
³⁰ brain and spinal cord. Neuronal death and gross volume loss has also been reported in the
³¹ hypothalamus in ALS ([Gorges et al., 2017](#)) ([Gabery et al., 2021](#)) ([Christidi et al., 2019](#)).
³² To measure such changes, methods for *in vivo* MRI segmentation of the hypothalamus and
³³ fornix include deep learning ([Billot et al., 2020](#)), seed growing techniques ([Wolff et al., 2018](#)),
³⁴ and manual segmentation ([Gorges et al., 2017](#)). There is a need to develop and distribute
³⁵ open-source atlases of these structures for more accurate and standardised segmentation. Here,
³⁶ we present the Open-Source Hypothalamic-ForniX (OSHy-X) atlases and tool for multi-atlas
³⁷ fusion segmentation for 3T and 7T. OSHy-X is an atlas repository and containerised Python
³⁸ script that automatically segments the hypothalamus and fornix at 3T and 7T in both T1w
³⁹ and T2w scans.

Methodology

Atlas

Twenty atlases were derived from manual segmentation of the hypothalamus-fornix, conducted by two tracers familiar with the hypothalamus and fornix (Chang & Shaw, 2021). Ten non-neurodegenerative disease participants and ten patients with ALS were selected at random from within the larger datasets of the EATT4MND and 7TEA studies for the tracing. Details of the acquisition parameters have been outlined previously (Chang et al., 2022).

Tool

A summary of the pipeline is illustrated in Figure 1. The user can specify the contrast (T1w/T2w) of the atlases used, the field strength (3T/7T) and any pre-processing steps. OSHy-X utilises Joint Label Fusion (JLF) (Wang et al., 2013) from Advanced Normalization Tools (ANTs; v2.3.1) for the registration (Avants et al., 2008) of atlases and segmentation of the target image. B1+ bias field inhomogeneity correction is performed using MriResearchTools (v0.5.2). Denoising and cropping are performed using ANTs in Python (ANTsPy; v0.2.0).

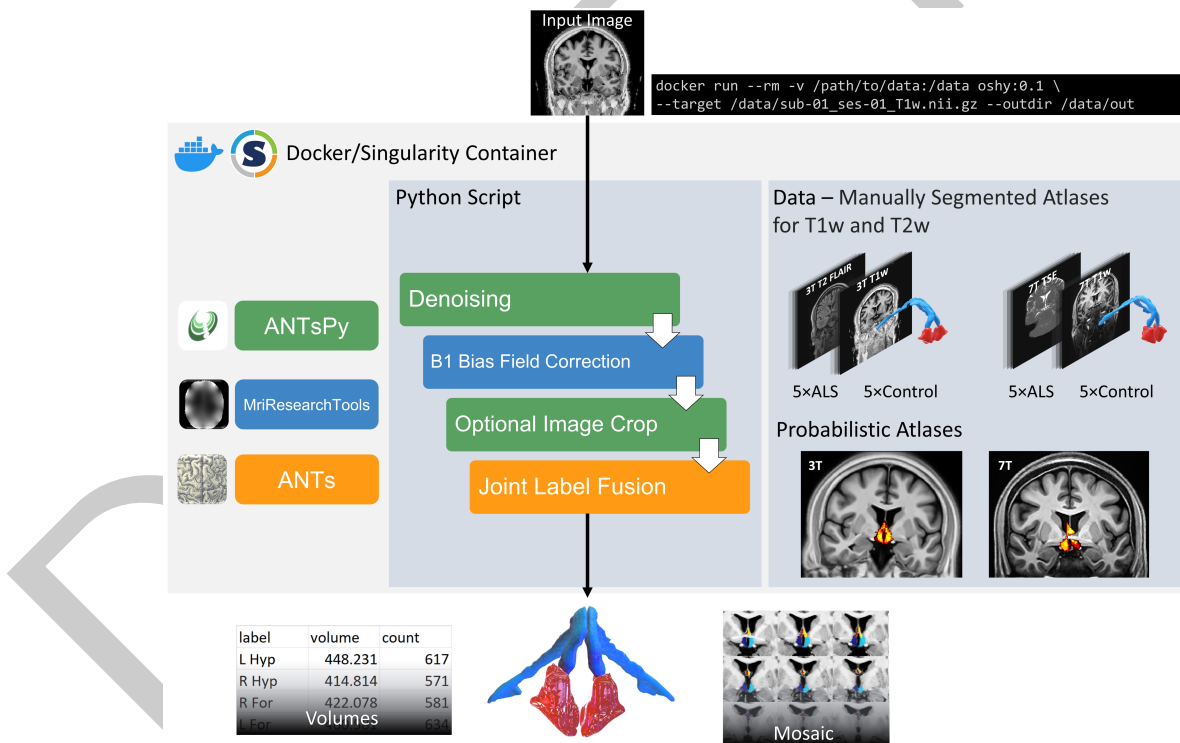


Figure 1: Pipeline overview of the OSHy-X segmentation tool. Users input a target image via a one-line command, and the pipeline produces hypothalamus and fornix labels, their volumes, and a mosaic visualisation of the segmentations. The pipeline and data are encapsulated within a Docker or Singularity container.

54 Performance

55 **Figure 2** visually compares the differences in the segmentation of a representative non-
 56 neurodegenerative disease participant using manual segmentation and JLF using leave-one out
 57 cross validation. Overall, JLF tends to under-segment throughout the hypothalamus and fornix.
 58 To a lesser extent, JLF tends to over-segment the anterior and lateral hypothalamus and the
 59 body of the fornix.

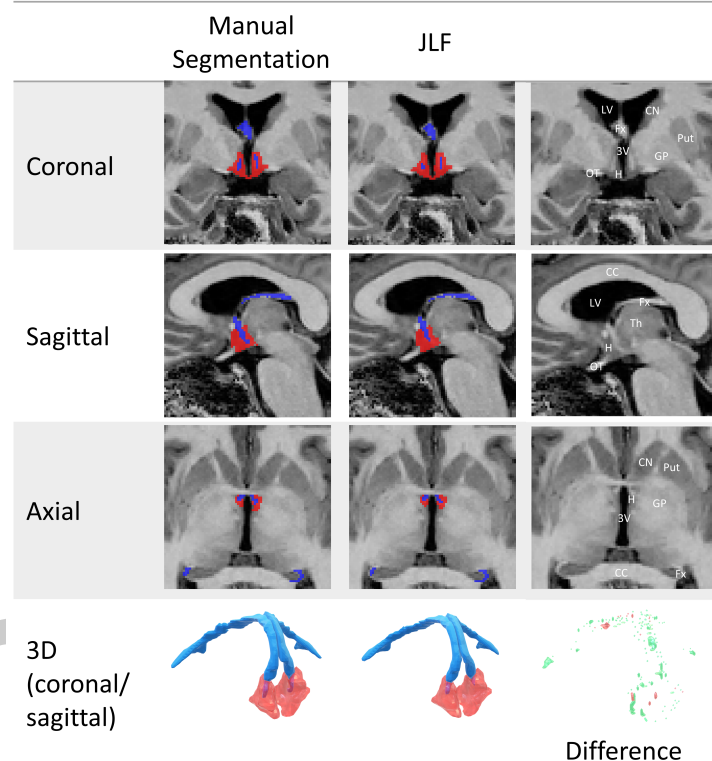


Figure 2: Visualisation of segmentation performance between manual segmentation and JLF. The hypothalamus is shown in red and the fornix in blue. The first three rows show segmentation in coronal, sagittal and axial planes; a 3D rendering of the structures is illustrated in the fourth row. The difference between JLF and manual segmentation illustrates over-segmented (red) and under-segmented (green) areas.

60 Dice overlaps ([Figure 3](#)) and (ICC; 2-way fixed-rater mixed effects model with single measure-
 61 ment) between the two raters indicate excellent segmentation accuracy. The left and right
 62 hypothalamus received scores of 0.90 (0.66-0.98 CI) and 0.91 (0.68-0.98 CI). The left and
 63 right fornix received scores of 0.97 (0.87-0.99 CI) and 0.68 (0.13-0.91 CI).

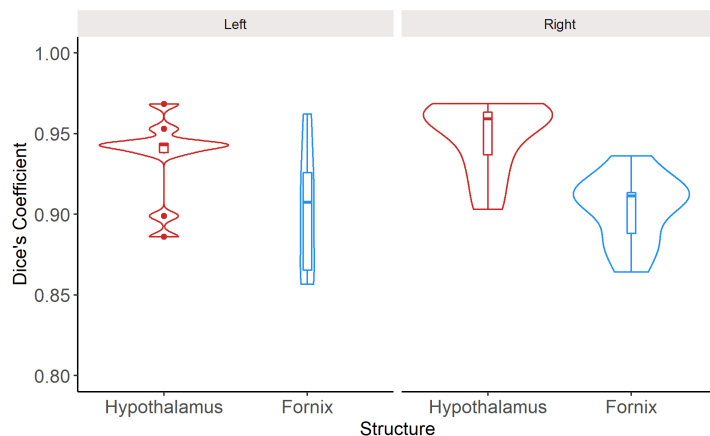


Figure 3: Dice overlaps between two raters for the left and right lobes of the hypothalamus and fornix. The median Dice's coefficient for the left and right hypothalamus is 0.94 (0.01 IQR) and 0.96 (0.03 IQR). The median Dice's coefficient for the left and right fornix are 0.91 (0.06 IQR) and 0.91 (0.03 IQR).

64 In comparison to a deep learning method for segmentation (Billot et al., 2020) (available in
 65 FreeSurfer v7.2), we found that JLF has higher Dice overlaps with the manual segmentations
 66 for both 3T and 7T (Figure 4). Additionally, we found that compared to cropped priors,
 67 whole-brain priors for JLF offers modest benefits to segmentation accuracy at 3T, but significant
 68 performance benefits at 7T compared to the deep learning method. While whole brain instead
 69 of cropped priors for JLF improves segmentation performance, computational time increases
 70 prohibitively.

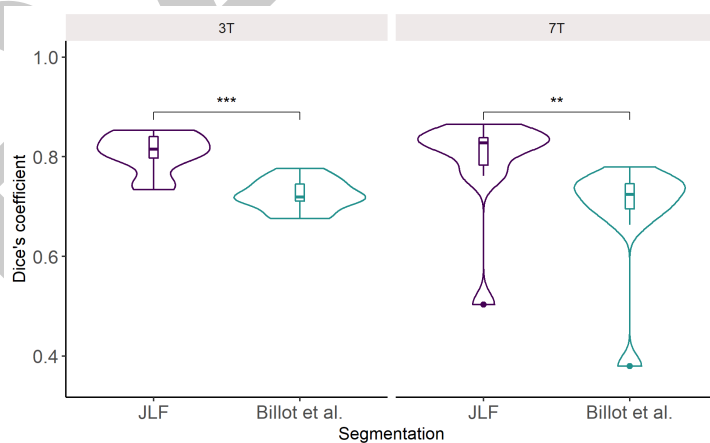


Figure 4: Dice overlaps of JLF with whole-brain priors and deep learning hypothalamic segmentation methods with manual segmentations. The median Dice's coefficient for JLF with 3T and 7T inputs are 0.82 (0.04 IQR) and 0.83 (0.06 IQR). The median Dice's coefficient for the deep learning method with 3T and 7T inputs are 0.72 (0.03 IQR) and 0.72 (0.05 IQR). In both 3T and 7T field strengths, JLF outperforms the deep learning method (Wilcoxon rank sum test; p<0.005 and p<0.05).

71 Availability

72 The OSHy-X atlas is freely available at (<https://osf.io/zge9t>) and the tool is available via the
 73 Neurodesk data analysis environment (<https://neurodesk.github.io>) or as a Docker/Singularity
 74 container (<https://github.com/Cadaei-Yuvxvs/OSHy-X>).

75 Acknowledgements

76 We thank all individuals who took part in the studies.

77 Funding for EATT4MND was provided by Wesley Medical Research (The Wesley Hospital,
78 Brisbane) and The Faculty of Medicine, The University of Queensland.

79 The authors acknowledge the facilities and scientific and technical assistance of the National
80 Imaging Facility, a National Collaborative Research Infrastructure Strategy (NCRIS) capability,
81 at the Centre for Advanced Imaging, The University of Queensland. This research was under-
82 taken with the assistance of resources and services from the Queensland Cyber Infrastructure
83 Foundation (QCIF). The authors gratefully acknowledge Aiman Al Najjer, Nicole Atcheson,
84 Anita Burns, Saskia Bollmann, and Amelia Celsis for acquiring data.

85 JC is supported by the UQ Graduate School Scholarship (RTP) and the Motor Neuron
86 Disease Australia Phd top-up scholarship grant. STN is supported by a FightMND Mid-Career
87 Fellowship. MB acknowledges funding from the Australian Research Council Future Fellowship
88 grant FT140100865. MB and SB acknowledge the ARC Training Centre for Innovation in
89 Biomedical Imaging Technology (CIBIT). TS is supported by a Motor Neurone Disease Research
90 Australia (MNDRA) Postdoctoral Research Fellowship (PDF2112).

91 References

- 92 Avants, B. B., Epstein, C. L., Grossman, M., & Gee, J. C. (2008). Symmetric diffeomorphic
93 image registration with cross-correlation: Evaluating automated labeling of elderly and
94 neurodegenerative brain. *Medical Image Analysis*, 12(1), 26–41. <https://doi.org/10.1016/j.media.2007.06.004>
- 96 Billot, B., Bocchetta, M., Todd, E., Dalca, A. V., Rohrer, J. D., & Iglesias, J. E. (2020).
97 Automated segmentation of the hypothalamus and associated subunits in brain MRI.
98 *NeuroImage*, 223, 117287. <https://doi.org/10.1016/j.neuroimage.2020.117287>
- 99 Chang, J., & Shaw, T. B. (2021). *Open source hypothalamic-ForniX (OSHy-X) atlases
100 and segmentation tool for 3T and 7T* [Online Database]. Available from <https://osf.io/zge9t/>. Accessed: 8 December 2021. <https://doi.org/10.17605/osf.io/zge9t>
- 102 Chang, J., Shaw, T. B., Holdom, C. J., McCombe, P. A., Henderson, R. D., Salvado, O., Barth,
103 M., Guo, C. C., Ngo, S. T., Steyn, F. J., & For the Alzheimer's Disease Neuroimaging
104 Initiative. (2022). *Lower hypothalamic volume with lower BMI is associated with shorter
105 survival in patients with ALS* [Unpublished Work].
- 106 Christidi, F., Karavasilis, E., Rentzos, M., Velonakis, G., Zouvelou, V., Xirou, S., Argyropoulos,
107 G., Papatriantafyllou, I., Pantolewn, V., Ferentinos, P., Kelekis, N., Seimenis, I.,
108 Evdokimidis, I., & P. B. (2019). Hippocampal pathology in amyotrophic lateral sclerosis:
109 Selective vulnerability of subfields and their associated projections. *Neurobiology of Aging*,
110 84, 178–188. <https://doi.org/10.1016/j.neurobiolaging.2019.07.019>
- 111 Gabery, S., Ahmed, R. M., Caga, J., Kiernan, M. C., Halliday, G. M., & Petersén, Å. (2021).
112 Loss of the metabolism and sleep regulating neuronal populations expressing orexin and
113 oxytocin in the hypothalamus in amyotrophic lateral sclerosis. *Neuropathology and Applied
114 Neurobiology*. <https://doi.org/10.1111/nan.12709>
- 115 Gorges, M., Vercruyse, P., Müller, H. P., Huppertz, H. J., Rosenbohm, A., Nagel, G., P,
116 P. W., Petersén, Å., Ludolph, A. C., Kassubek, J., & Dupuis, L. (2017). Hypothalamic
117 atrophy is related to body mass index and age at onset in amyotrophic lateral sclerosis.
118 *Journal of Neurology, Neurosurgery, and Psychiatry*, 88(12), 1033–1041. <https://doi.org/10.1136/jnnp-2017-315795>

- 120 Wang, H., Suh, J. W., Das, S. R., Pluta, J. B., Craigie, C., & Yushkevich, P. A. (2013).
121 Multi-atlas segmentation with joint label fusion. *IEEE Transactions on Pattern Analysis
122 and Machine Intelligence*, 35(3), 611–623. <https://doi.org/10.1109/tpami.2012.143>
- 123 Wolff, J., Schindler, S., Lucas, C., Binninger, A. S., Weinrich, L., Schreiber, J., Hegerl, U.,
124 Möller, H. E., Leitzke, M., Geyer, S., & Schönknecht, P. (2018). A semi-automated
125 algorithm for hypothalamus volumetry in 3 tesla magnetic resonance images. *Psychiatry
126 Research. Neuroimaging*, 277, 45–51. <https://doi.org/10.1016/j.psychresns.2018.04.007>

DRAFT